



Oligomer and highly oxygenated organic molecule formation from oxidation of oxygenated monoterpenes emitted by California sage plants

Archit Mehra¹, Jordan E. Krechmer², Andrew Lambe², Chinmoy Sarkar³, Leah Williams², Farzaneh Khalaj³, Alex Guenther⁴, John Jayne², Hugh Coe^{*1}, Douglas Worsnop², Celia Faiola^{3,5}, Manjula Canagaratna^{*2}

5 ¹Centre for Atmospheric Science, School of Earth and Environmental Sciences, The University of Manchester, Manchester, UK

²Center for Aerosol and Cloud Chemistry, Aerodyne Research Inc., Billerica, Massachusetts, USA

³Department of Ecology and Evolutionary Biology, University of California, Irvine, Irvine, California, USA

⁴Department of Earth System Science, University of California Irvine, Irvine, California, USA

⁵Department of Chemistry, University of California, Irvine, Irvine, California, USA

10 *Correspondence to Manjula Canagaratna (mrcana@aerodyne.com) and Hugh Coe (hugh.coe@manchester.ac.uk)

Abstract

Plants emit a diverse range of biogenic volatile organic compounds (BVOC) whose oxidation leads to secondary organic aerosol (SOA) formation. The majority of studies of biogenic SOA have focused on single or simple multi-component BVOC mixtures thought to be representative of Northern Hemispheric deciduous or mixed forest conditions. Gaps remain in our understanding of SOA formation from complex mixtures of real plant emissions in other environments.

Towards the goal of understanding SOA in other regions, we conducted the first comprehensive study of SOA from oxygenated monoterpenes. These are the dominant emissions from the most common plant species in southern California's coastal sage ecosystem: black sage (*Salvia mellifera*) and California sagebrush (*Artemisia californica*).

15 Emissions from sage plants, and single compounds representing their major emissions (camphor, camphene and eucalyptol), were oxidised in an Aerodyne potential aerosol mass oxidation flow reactor (PAM-OFR). The chemical composition of SOA was characterised using a high-resolution time-of-flight iodide-anion chemical-ionization mass spectrometer equipped with a Filter Inlet for Gases and AEROSols (FIGAERO-I-HR-ToF-CIMS) under low and medium-NO_x conditions.

25 SOA from oxygenated monoterpenes showed higher order oligomer content and a greater presence of highly oxygenated organic molecules (HOM) than non-oxygenated monoterpenes, with HOM contributing 27 – 47 % and 12-14 % of SOA product signal from oxygenated and non-oxygenated monoterpenes, respectively. This study highlights the potential importance of oxygenated monoterpene emissions for SOA formation in woody shrub ecosystems.

1. Introduction

30 Secondary organic aerosol (SOA) formed from the oxidation of volatile organic compounds (VOCs) contributes 50-85 % of organic aerosol in the atmosphere (Jimenez et al., 2009). VOCs from biogenic emission sources (BVOCs) are estimated to contribute 75 – 90 % of total VOC (Guenther et al., 1995; Lamarque et al., 2010, Carlton et al., 2009; Claeys et al., 2004). BVOC oxidation by reaction with ozone, hydroxyl radical or nitrate radical has been estimated to contribute up to 50 % of SOA worldwide (Chung and Seinfeld, 2002; Hoffmann et al., 1997) having implications for air quality, climate and human health (Chung and Seinfeld, 2002; Fiore et al., 2012; Forster et al., 2007; Lohmann and Feichter, 2005).

35 Formation of highly oxygenated organic molecules (HOM) has been identified as a pathway for new particle formation and growth of SOA (Bianchi et al., 2019). Recent work has shown that alongside HOM formation from ozonolysis (Quéléver et al., 2019), hydroxyl radical oxidation of monoterpenes is a large source of HOM (Berndt et al., 2016). Oligomerisation is another key pathway to formation of SOA and has been identified as important for monoterpenes including α -pinene and limonene (Hall and Johnston, 2011; Kourtchev et al., 2016; Kundu et al., 2012; Putman et al., 2011; Tolocka et al., 2004). Uncertainties remain in the relative importance and sensitivity to anthropogenic conditions of the different SOA formation pathways alongside their relevance in other BVOC systems.

40 Isoprene and α -pinene are globally the most abundant aerosol forming BVOCs emitted from vegetation and forests and thus have been the focus of many studies on SOA formation and composition (Carlton et al., 2009; Després et al., 2012; Guenther et al.,



2012; Kroll, 2006; Zhang et al., 2015). However, these are only a subset of over 1700 BVOCs which have been identified from plant emissions (Dudareva et al., 2006). Though most of these are thought to have a negligible contribution on the global scale, they could be a major contributor in specific ecosystems and thus important on local scales. Despite this diversity, chemical composition of SOA from the majority of these BVOCs remains unknown. Real plant emissions are mixtures of many BVOCs, yet it remains unclear if the compounds currently used as proxies for BVOCs are adequate to describe SOA chemistry of plants globally (Faiola et al., 2018).

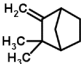
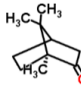
Real plant emissions have been used as atmospherically relevant VOC mixtures in various studies (Faiola et al., 2015, 2019; Hao et al., 2009, 2011; Joutsensaari et al., 2005, 2015; Mentel et al., 2009; Vanreken et al., 2006; Yli-Pirilä et al., 2016; Ylisirniö et al., 2019; Zhao et al., 2017), however, most of these used conifers or broad-leaved trees. Comparison of pine species has shown that thresholds of new particle formation (NPF) from plant emissions are lower than that for α -pinene alone, and plants with a larger proportion of oxygenated VOCs (OVOCs) have the lowest thresholds (Mentel et al., 2009). For mainly isoprene emitting plants, SOA yields from co-emitted VOCs were less than expected from single-VOC data, suggesting that isoprene inhibits SOA formation (Wyche et al., 2014). Furthermore, recent incorporation of terpene complexity into a box model has demonstrated enhancements of 1.5-2.3 in SOA mass yields from Scots pine, relative to the commonly used model monoterpene α -pinene (Faiola et al., 2018). Though studies of SOA from real plant emissions are limited, all results show pronounced differences between plants and single components. This suggests that simplification of BVOC complexity may be responsible for model under-estimates of organic aerosol mass loadings in dry shrubland areas of the western United States (Carlton et al., 2018).

The impact of mixing BVOCs on SOA has been recently studied using mixtures of α -pinene and isoprene, and results have shown that isoprene can suppress the mass yield derived from monoterpenes through oxidant scavenging (McFiggans et al., 2019). Utilisation of detailed chemical composition enabled attribution of this effect to a reduction in yield of low volatility HOM products which form SOA, relative to their yields during single VOC oxidation (McFiggans et al., 2019). This study demonstrates the utility of detailed chemical composition for deconvolution of SOA from complex mixtures. Despite these findings, studies to date have lacked adequate characterisation of differences in chemical composition between SOA from plants and single precursors.

Relative proportions of different BVOCs in the atmosphere is a function of both the plant species and environmental factors. Thus VOC mixtures vary regionally and globally, making the need to understand SOA formation from different precursors and mixtures vital for application in regions with different BVOC source profiles (Guenther, 2013). For example, at some agricultural locations in California, oxygenated monoterpene emissions and ambient concentrations were higher than anthropogenic and monoterpene VOCs (Gentner et al., 2014) suggesting that they may be important for SOA formation in this region.

In this study we investigate the VOC emission profile of two species of plant native to California: black sage (*Salvia mellifera*, Sage herein) and California sagebrush (*Artemisia californica*, Artemisia herein) and subsequent SOA formation from hydroxyl radical oxidation of these VOCs in an oxidation flow reactor (OFR) under low and medium NO_x conditions. On the basis of the measured emission profiles of these species, we also studied SOA formed from individual VOCs which were major contributors, camphene, camphor and eucalyptol (Table 1).

Though terpenoid emissions of sage plants into the atmosphere were reported in the mid-1970s (Tyson et al., 1974) and they have been considered by plant scientists for their ecological function (Karban et al., 2014), these are the first detailed SOA composition measurements from these plants and the first study of woody shrubs, which are the dominant vegetation type in many landscapes including coastal sage scrub, shrub lands and chaparral. Atmospherically relevant studies of the VOC precursors alone have focused on gas phase reaction rates and chemistry but not looked into the SOA (Ceacero-Vega et al., 2012; Gaona-Colmán et al., 2017a). Our results show high HOM and oligomer formation from oxygenated monoterpenes which dominate the emission profile of California sage plants.

Precursor	Formula	Structure	kOH ($\text{cm}^3 \text{molecule}^{-1} \text{s}^{-1}$)
Camphene	$\text{C}_{10}\text{H}_{16}$		5.95E^{-11} (Gaona-Colmán et al., 2017b)
Camphor	$\text{C}_{10}\text{H}_{16}\text{O}$		3.8E^{-12} (Ceacero-Vega et al., 2012)



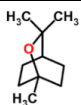
Eucalyptol (1,8-cineole)	$C_{10}H_{18}O$		$1.11E^{-11}$ (Corchnoy and Atkinson, 1990)
-----------------------------	-----------------	---	---

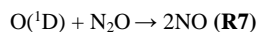
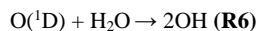
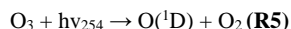
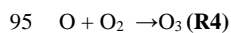
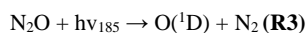
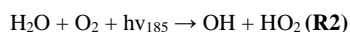
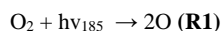
Table 1 VOCs investigated in this study

2. Experimental Methods

85 2.1. Oxidation of VOCs and SOA Production

SOA particles were generated by the OH oxidation of VOCs in an Aerodyne Potential Aerosol Mass (PAM) oxidation flow reactor (OFR) (Lambe et al., 2011) affording short experimental timescales and the ability to generate consistent and reproducible oxidation conditions. Plant emissions were sampled from an external plant chamber into the OFR using an eductor. Eucalyptol was injected into the OFR through a length of Teflon tubing using a syringe pump, prior to evaporation into N_2 carrier gas. Camphene or camphor vapour were introduced by flowing N_2 over solid camphene or camphor placed in a Teflon tube.

In the OFR, OH, HO_2 and NO were generated via the following reactions:



All experiments were carried out at room temperature (approximately 26 °C), relative humidity of 35 % and constant gas flow of 10 standard litres per minute (SLM) through the OFR, including injection of ~3 % N_2O at the inlet to generate NO in a subset of experiments (Lambe et al., 2017; Peng et al., 2018). The OFR was run in OFR185 mode which uses 185 nm photons to generate radicals by the reactions outlined above, and under these conditions the estimated OH exposures were in the range of $(1.5-1.7) E^{12}$ molecules $cm^{-3} s^{-1}$. In experiments where N_2O was added to the OFR, the NO: HO_2 ratio was approximately 0.5 as calculated using an adapted version of the OFR photochemical box model described in (Li et al., 2015) and (Peng et al., 2015). Between experiments, the flow reactor was flushed with humidified synthetic air at full lamp power for 12-36 hours until the particle mass generated was reduced to background concentrations ($< 0.5 \mu g m^{-3}$), measured by a scanning mobility particle sizer (SMPS) and an aerosol mass spectrometer (AMS). Instrument and OFR backgrounds were determined using $N_2 + O_2$ injection under lights off/on, with/without precursor injection. The results presented here are for low NO_x ($[NO] < 0.1$ ppb) and medium NO_x ($[NO] > 1$ ppb, $[NO]: [HO_2] = 0.5$) conditions.

110 2.2. FIGAERO-I-HR-ToF-CIMS Measurements

A time of flight chemical ionisation mass spectrometer (Lee et al., 2014) using an iodide-anion ionisation system was coupled with a filter inlet for gases and aerosols (FIGAERO) (Lopez-Hilfiker et al., 2014) for detection of both gas and particle phase composition (I-CIMS herein). The gas phase inlet consisted of a piece of 0.5 m long ¼" O.D. PFA tubing from which the I-CIMS sub-sampled 2 SLM. The aerosol phase inlet consisted of 0.5 m stainless steel tube through which 2 SLM were pulled over a Teflon filter. The sample flow (gas or aerosol) enters an ion molecule reaction region (IMR) which was maintained at a pressure of 100 mbar using a pump fitted with a pressure controller. I reagent ion was made by flowing N_2 over a permeation tube containing methyl iodide (CH_3I), mixing that flow with a humidified N_2 flow from a bubbler, and then ionising with a Po-210 source. Particle mass concentrations were monitored using a TSI Scanning Mobility Particle Sizer (SMPS, TSI, Model 3080) and collection time on the FIGAERO filter was varied to ensure hundreds of nanograms of aerosol in each sample for the different precursors. The FIGAERO thermal desorption cycle consisted of a 15-minute temperature ramp to 200 °C, a hold at that temperature for 10 minutes and then cooling down over 15 minutes.

Data analysis is performed using the Tofware package (version 3.1.0) running in the Igor Pro (WaveMetrics, OR, USA) environment. Time of flight values were converted to mass-to-charge ratios in the I-CIMS data using a calibration curve based on



125 the times for I^- , $I.H_2O^-$ and I_3^- . The instrument was operated at a ~ 4000 Th/Th resolving power. Further analysis was carried out in custom Python 3 procedures using the packages Pandas, Matplotlib and Numpy.

130 While the FIGAERO is capable of providing information about both gas and particle phases, the gas phase I-CIMS spectra obtained during the medium NO_x experiments were complicated by the presence of high nitric acid formed in the OFR from the N_2O precursor (Lambe et al., 2017; Peng et al., 2018). High nitric acid depletes the I^- reagent ion to form NO_3^- , which subsequently acts as an additional reagent ion and complicates interpretation of the observed CIMS spectra. Thus, the gas phase measurements are deemed unsuitable for the comparison of medium and low NO_x conditions and the HR analysis of the I-CIMS spectra has been carried out only for the particle phase FIGAERO data. This data provides thermal desorption profiles which have been previously used to draw conclusions about the volatility distribution of ions. However, in this study we do not make use of this owing to the additional complexity associated with calibration of the volatility and uncertainties with thermal decomposition (Bannan et al., 2019; Schobesberger et al., 2018; Stark et al., 2017) and instead integrate these desorption profiles in order to compare the overall composition of the different precursors. For all plant and VOC experiments, $> 70\%$ of observed product signal was assigned with molecular formulae and these ions are used for analysis herein.

140 Quantification of highly oxidised species measured by I-CIMS is challenging due to the lack of availability of standards for many of the observed products. Previous attempts at quantification have used functional group dependencies, collision limit sensitivities or those derived from ion-adduct declustering scans (Lopez-Hilfiker et al., 2016). Experimental limitations exist in the use of these techniques, meaning that quantification remains a challenge (Riva et al., 2019) thus in this study we utilise observed ion signal intensities without accounting for species-dependent differences in instrument sensitivity.

2.3. TD-GC-FID/ToF-MS VOC Measurements

145 Gas-phase VOC profiles during the SOA experiments using real plants were characterized at the inlet of the PAM flow reactor. Samples were collected by trapping VOCs onto multi-bed adsorbent cartridges containing Carbograph 5TD and Tenax TA adsorbents (Markes International, part # C2-AXXX-5149). Sampling lines were conditioned for a minimum of 10 minutes to minimize VOC line losses before attaching adsorbent cartridges. Air was pulled through duplicate cartridges with a sampling pump at $300\text{ cm}^3\text{ min}^{-1}$ for 20 minutes. On days where experiments were run using real plant emissions, duplicate cartridges were collected at the PAM inlet at least twice per day. Cartridges were shipped overnight to UCI on ice for offline analysis on a thermal-desorption gas chromatograph interfaced with a flame ionization detector and a time-of-flight mass spectrometer (TD-GC-ToF-MS: TD-Series 2 Unity + Ultra, Markes International; 7890B Agilent GC-FID; BenchToF-Select MS, Markes International). Compounds were identified using the 70 eV MS spectra by comparing them with compounds in the NIST library. Terpene mixing ratios at the PAM inlet were quantified using the FID signal as described elsewhere using the effective carbon number concept (Faiola et al., AMT, 2012).

2.4. AMS Measurements

155 SOA composition was continuously measured at the PAM outlet with a high-resolution time-of-flight aerosol mass spectrometer (HR-LToF-AMS; Aerodyne Research, Inc.) described in detail elsewhere (Canagaratna et al., 2007; DeCarlo et al., 2006). Briefly, the HR-LToF-AMS collimates sub-micron particles into a narrow beam with an aerodynamic lens. The particle beam is directed onto a vaporizer plate at $600\text{ }^\circ\text{C}$ to vaporize non-refractory components. Volatilized fragments are ionized with 70 eV electron impact ionization and detected with a Long-ToF mass spectrometer (Tofwerk, resolving power 4000 Th/Th) where the ionized fragments are separated by mass. The detection efficiency was calibrated with monodisperse ammonium nitrate particles generated with a constant output atomizer (TSI, Model 3076) and a differential mobility analyser (DMA, TSI, Model 3080). AMS data was analysed using the Squirrel (v1.60P) and Pika (v1.20P) ToF-AMS toolkits in Igor Pro (v6.37; Wavemetrics, Inc.). Medium NO_x experiments had a large N_2O interference with CO_2 and thus O:C are not presented.

165



170 3. Results & Discussion

3.1. VOC emissions from Plants

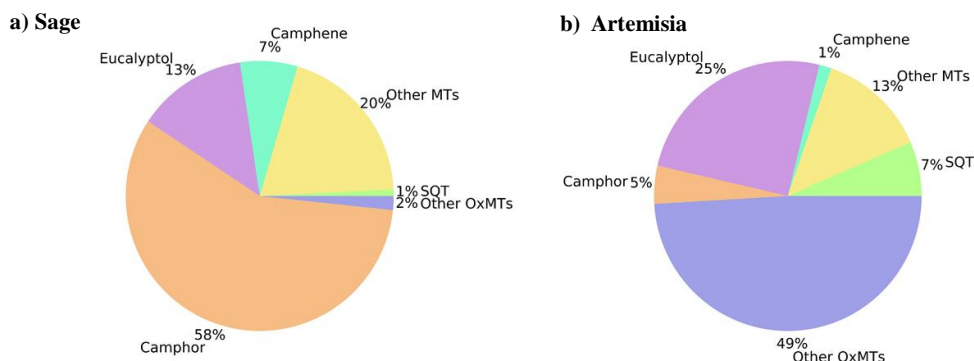


Figure 1 VOC emission profiles of a) Sage and b) Artemisia where OxMTs are oxygenated monoterpenes, MTs are monoterpenes and SQT are sesquiterpenes.

175 Figure 1 shows a single snapshot of VOC composition from these plants to note the main features relevant for the SOA composition measured with I-CIMS. Both Sage and Artemisia plant emission profiles are dominated by oxygenated monoterpenes (73 and 79 %, respectively), the least studied BVOC type (Goldstein and Galbally, 2007), while other monoterpenes have a small contribution (20 and 13 %, respectively). For Artemisia, eucalyptol contributes a larger proportion of the signal than camphor (25 and 5 %, respectively) while camphor alone dominates the emission profile of Sage (58 %). Artemisia has a large contribution (49 %) from other oxygenated monoterpene species. Speciation of VOC emissions vary between the two plants and the detailed VOC profiles and SOA yields will be presented in a separate paper. Of the monoterpenes, composition of SOA from camphene is least well characterised due to its low reactivity with ozone, however it is highly reactive with hydroxyl radical (Gaona-Colmán et al., 2017a) and is thus studied in detail in this paper. The following section focuses on characterisation and comparison of SOA from photooxidation of camphor, camphene and eucalyptol alongside SOA produced from photooxidation of the Sage and Artemisia plant emissions under low and medium-NO_x conditions.

185

3.2. Overview of SOA Composition

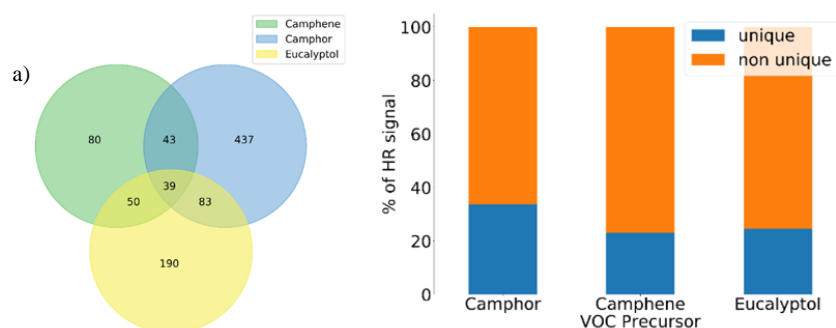


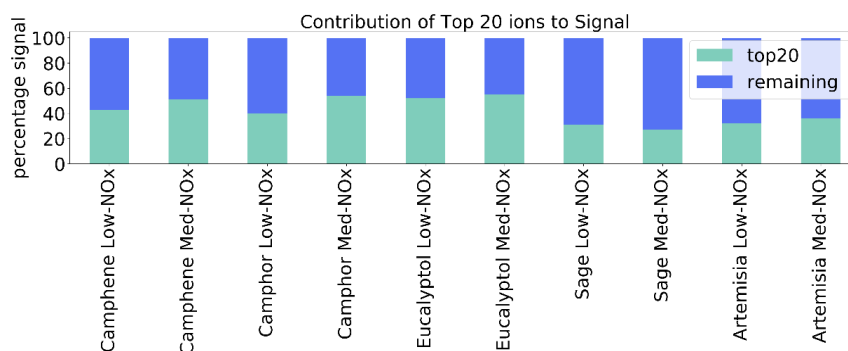
Figure 2 a) Comparison of ions from peak lists of individual VOC precursors (no. of ions shown in Venn) and b) contribution of unique and non-unique products to total signal derived from Venn under low-NO_x conditions

Here we utilise the ions identified in each experiment to carry out a qualitative comparison of SOA composition between the different VOC precursors and plants. Figure 2a shows a Venn diagram of the number of distinct molecular formulas used in the high-resolution ion peak lists for camphene, camphor, and eucalyptol spectra. A majority of the assigned ions are unique to each of the precursors, and a small number of ions are non-unique (i.e. are present in the mass spectra of all 3 of the precursors). The relatively small number of non-unique ions (39) formed from all the precursors contributes to > 70 % of the product signal observed (Figure 2b). Unique ion signal is minor and is distributed across many more ions (80-437) (Figure 2a). Due to the relatively low signal intensity of these individual unique ions, it is not deemed suitable to use them as markers, particularly as

190



195 there is ambiguity in their assignment under the limited resolution of the mass spectrometer and potential artefacts due to thermal decomposition caused by the FIGAERO. The percentage of signal from the 20 highest intensity ions (Figure 3) shows that the complexity of SOA from plants is greater than that of single components where up to 40 - 60 % of the product signal can be attributed to the top 20 ions. The top 20 ions observed under low and medium-NO_x conditions are listed in Table S1 and S2, respectively.



200

Figure 3 Contribution of Top 20 ions to observed product signal

3.3 HOM & Oligomer Formation

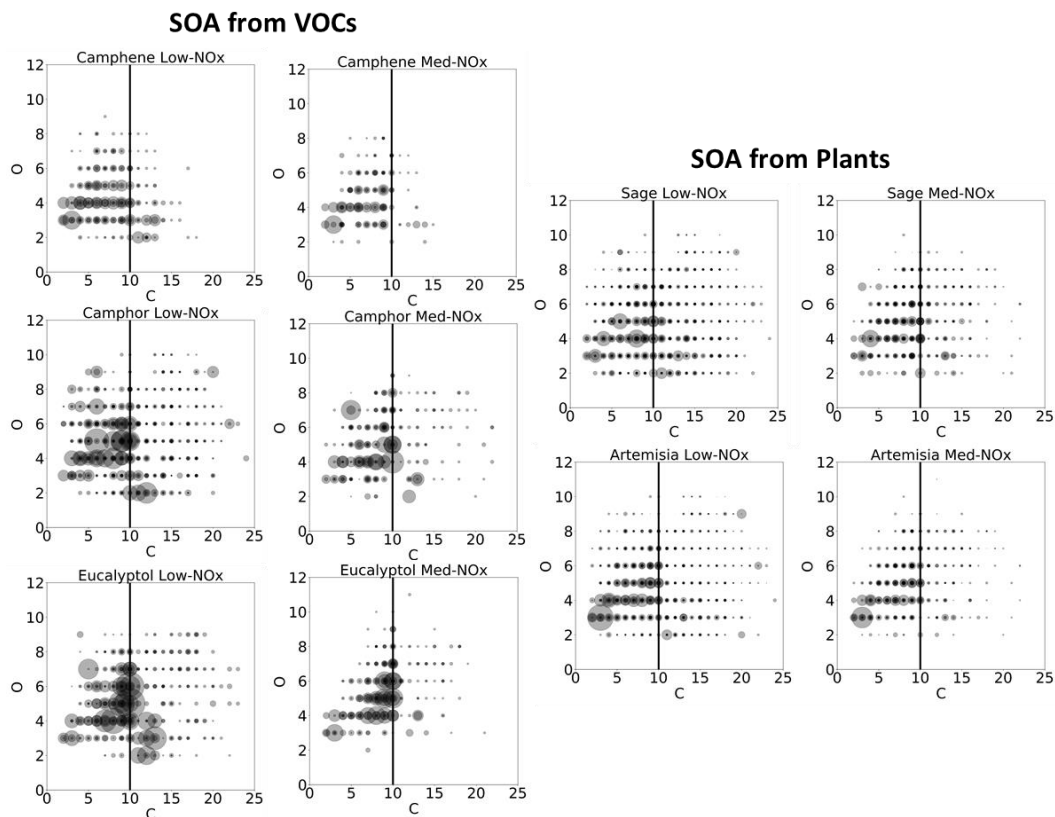


Figure 4 Carbon vs. Oxygen Plot for Aerosol Phase Composition under low and medium NO_x conditions for VOC precursors and plants (vertical black line separates monomers and oligomers in carbon number space and symbols are proportional to ion intensity).



205 Figure 4 plots the ions observed during all experiments according to their carbon and oxygen numbers. This figure highlights
 some of the differences in the SOA spectra between the single precursors and the plant emissions. SOA from the oxygenated
 monoterpenes (camphor and eucalyptol) has lower O:C than that of camphene (Table 2), although their products are generally
 higher mass (Figure S1). Oxidation of camphene yields mainly small, low mass (Figure S1), molecular fragmentation products
 (<C₁₀) as compared with camphor and eucalyptol which have many more products at higher carbon numbers. The bulk of the signal
 210 for camphene SOA is spread amongst fragmentation products, while for camphor it is a mixture between fragmentation and those
 retaining the carbon backbone of the precursor (Figure 2, vertical black line). In eucalyptol SOA, a large proportion of signal can
 be attributed to oxidised C₁₀ products which form with no fragmentation of the carbon backbone, and there is a larger contribution
 from oligomers (≥ C₁₁).

Precursor	Condition	O:C I-CIMS	O:C AMS	C _x H _y O _z
Camphene	Low NO _x	0.69	0.70	C _{7.26} H _{9.85} O _{4.03}
	Medium NO _x	0.74	-	C _{6.63} H _{9.7} N _{0.12} O _{4.21}
Camphor	Low NO _x	0.66	0.64	C _{8.97} H _{12.34} O _{4.8}
	Medium NO _x	0.66	-	C _{8.34} H _{11.98} N _{0.07} O _{4.71}
Eucalyptol	Low NO _x	0.58	0.52	C _{9.45} H _{13.09} O _{4.85}
	Medium NO _x	0.65	-	C _{8.47} H _{12.37} N _{0.01} O _{5.06}
Sage	Low NO _x	0.74	0.78	C _{9.54} H _{13.30} O _{4.52}
	Medium NO _x	0.66	-	C _{8.42} H _{12.34} N _{0.09} O _{4.66}
Artemisia	Low NO _x	0.67	0.74	C _{8.51} H _{11.79} O _{4.58}
	Medium NO _x	0.71	-	C _{7.62} H _{11.07} N _{0.06} O _{4.65}

Table 2 Bulk Composition of SOA from single component standards and plants

230 Despite different species contributing to the emissions profiles for the two plants, bulk composition and average molecular
 formulae are similar (Table 2). A potential explanation for this is the similar contributions from oxygenated monoterpenes (Figure
 1), which may have similar SOA characteristics despite different speciation. The monomer region of plant SOA (≤ C₁₀) can be
 attributed to fragmentation products from all VOCs. However, the presence of oligomers (≥ C₁₁) in the plant SOA is likely to be
 from products associated with the oxygenated monoterpenes as camphene shows few oligomer products (Figure 4).

235 Under medium-NO_x conditions the O:C of SOA was higher than under low-NO_x conditions for camphene, eucalyptol and
 Artemisia (Table 2). Though smaller carbon number SOA products are observed under medium-NO_x conditions for all except
 camphene, average molecular formula show that the average oxygen content is not altered, suggesting that further oxidation of
 fragmentation products continues under elevated NO_x (Table 2). It is also noted that oxidation of eucalyptol under low NO_x
 conditions yields larger products, and higher NO_x conditions give more similar SOA to other precursors. Fewer high carbon number
 products are observed under medium-NO_x conditions for all precursors, however this effect is more notable in the single component
 240 experiments than the plant SOA, where low and medium-NO_x conditions look largely similar (Figure 4). Under medium NO_x
 conditions, nitrogen containing products are observed, with largest contributions to signal in camphor (35 %), followed by Sage
 (30 %), camphene (28 %), Artemisia (19 %) and eucalyptol (7 %).

245

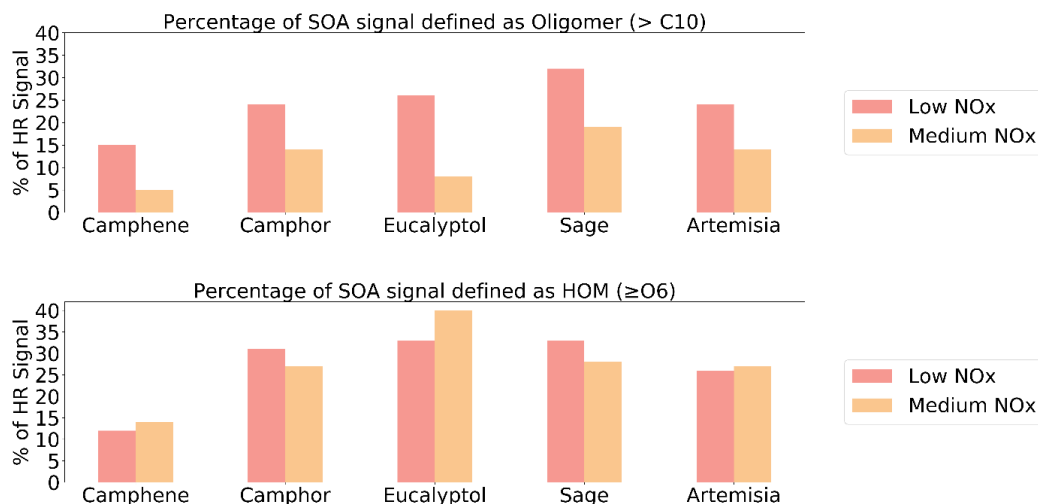


Figure 5 Comparison of the proportion of signal attributable to oligomeric species (top) and HOMs (bottom)

Two key pathways of SOA formation from BVOCs have been identified; formation of highly oxygenated organic molecules (HOM) (Bianchi et al., 2019; Ehn et al., 2014; Jokinen et al., 2014; Tu et al., 2016) and oligomerisation (Hall and Johnston, 2011; Kourtchev et al., 2016; Kundu et al., 2012; Putman et al., 2011; Tolocka et al., 2004). HOMs are defined here as ions which contain six or more oxygen atoms (Bianchi et al., 2019). Figure 6 shows the relative contributions of HOM and oligomer products to observed signal for the different precursors and plants, aiding in evaluation of the relative importance of different SOA formation pathways under low and medium NO_x conditions.

Our results show large contributions of HOM to total product signal from the oxygenated monoterpenes of up to 40 %, while contributions of HOM to camphene SOA are as low as 12-14 % (Figure 6). HOM show minimal differences in contribution to signal between low and medium-NO_x conditions, whereas oligomers show a decrease in all cases with NO_x addition. This suggests that HOM formation itself, a rapid intramolecular process, is not hindered by NO_x under these conditions, while NO hinders oligomerisation. Figure 6 also indicates that the oligomer content in SOA is highest for oxygenated monoterpenes. Previous studies of mixtures have shown oligomer content to be similar to that of α -pinene alone (Kourtchev et al., 2016). However, our results suggest that in low α -pinene emitting plant species such as Sage and Artemisia, other VOCs such as camphor and eucalyptol may become important for oligomer formation.

Recently Ylisirniö et al. (2019) have published FIGAERO-CIMS studies of α -pinene SOA from PAM-OFRR experiments. The proportion of HOM signal calculated from the α -pinene SOA spectra presented in (Ylisirniö et al., 2019) ranges from 41 % HOM at low OH exposure to 62 % at higher OH exposure. These HOM values are higher than those obtained in our experiment. However, there are differences in experimental conditions that complicate these comparisons. The conditions utilised in Ylisirniö et al (2019) used OFR254, which utilises both 185 nm and 254 nm photons, as opposed to OFR185 which was used in our experiments. In OFR254, HO₂ concentrations are lower than in OFR185; increased HO₂ under the OFR185 conditions utilised during our experiments may suppress HOM formation and explain the differences between the two experiments. Therefore, though more HOM is observed for α -pinene in Ylisirniö et al (2019), a true comparison would require these precursors to be run under the same conditions.

4. Conclusions & Implications

Emissions of VOCs from sage and Artemisia plants, widespread in California and much of the western United States, are different from that of other commonly studied plants such as conifers and broad-leaved trees, since emissions of oxygenated monoterpenes are the largest fraction. Here we have presented detailed chemical characterisation of SOA from Sage and Artemisia plants, from 2 oxygenated monoterpene precursors emitted by these species (camphor and eucalyptol) and from a monoterpene (camphene). Results show up to 40 % of product signal was from HOMs for the oxygenated monoterpene precursors and clear oligomerisation was observed. Under elevated NO_x conditions, HOM formation did not change significantly. However, oligomerisation was reduced for all precursors and plants.



280 Sage plants emit a mixture of BVOCs, and SOA formed from their emissions shows greater complexity than single components, though the majority of ions observed are generic monoterpene oxidation products emitted from all the investigated VOCs. Thus, constraining VOC contributions to SOA in complex mixtures remains a challenge. Our results clearly show that in the plant emission mixtures, HOMs can contribute up to 33 % of signal and oligomerisation continues to be a significant fraction of the SOA. This indicates that oxygenated monoterpenes may be key to understanding SOA in regions with many sage plants or other high oxygenated monoterpene emitting plant species.

285 This is the first detailed study of oxygenated monoterpene SOA chemistry using both single component standards and real plant emissions. Eucalypts, dominant emitters of eucalyptol, are present globally with many different species, and it is likely that they are globally important for SOA formation. Previously reported low thresholds of new particle formation from species containing high proportions of oxygenated monoterpenes (Mentel et al., 2009) could be explained by the high oligomer content of the SOA we have observed for these VOCs and in the mixtures. High oligomer content has been shown to influence particle viscosity by intra- and inter-molecular hydrogen bonding between oligomers (Huang et al., 2018), and thus our results could indicate very
290 different physicochemical properties for SOA generated from plants which contain high proportions of oxygenated monoterpenes.

5. Author Contributions

CF designed the experiments. Instrument deployment and operation were carried out by CF, AM, JEK, CS, LW and FK. AMS analysis was carried out by CF. AM carried out I-CIMS analysis and wrote the paper. AG and CS ran the volatile sample analysis. All co-authors discussed the results and commented on the manuscript.

295 6. Acknowledgements

Archit Mehra is fully funded by the Natural Environment Research Council (NERC) and acknowledges his funding through the NERC EAO Doctoral Training Partnership (NE/L002469/1) and CASE partnership support from Aerodyne Research Inc.

7. Competing Interests

The authors declare they have no conflicts of interest.

300 8. Data Availability

Data is available upon request from corresponding authors.

9. Supplement

Supplement is included.

10. References

305 Bannan, T. J., Le Breton, M., Priestley, M., Worrall, S. D., Bacak, A., Marsden, N. A., Mehra, A., Hammes, J., Hallquist, M., Alfarra, M. R., Krieger, U. K., Reid, J. P., Jayne, J., Robinson, W., Mcfiggans, G., Coe, H., Percival, C. J. and Topping, D.: A method for extracting calibrated volatility information from the FIGAERO-HR-ToF-CIMS and its experimental application, *Atmos. Meas. Tech.*, 12, 1429–1439, doi:10.5194/amt-12-1429-2019, 2019.

310 Berndt, T., Richters, S., Jokinen, T., Hyttinen, N., Kurtén, T., Otkjaer, R. V., Kjaergaard, H. G., Stratmann, F., Herrmann, H., Sipilä, M., Kulmala, M., Ehn, M., Otkjær, R. V., Kjaergaard, H. G., Stratmann, F., Herrmann, H., Sipilä, M., Kulmala, M. and Ehn, M.: Hydroxyl radical-induced formation of highly oxidized organic compounds, *Nat. Commun.*, 7, 13677, doi:10.1038/ncomms13677, 2016.

Bianchi, F., Kurtén, T., Riva, M., Mohr, C., Rissanen, M. P., Roldin, P., Berndt, T., Crouse, J. D., Wennberg, P. O., Mentel, T. F., Wildt, J., Junninen, H., Jokinen, T., Kulmala, M., Worsnop, D. R., Thornton, J. A., Donahue, N.,
315 Kjaergaard, H. G. and Ehn, M.: Highly Oxygenated Organic Molecules (HOM) from Gas-Phase Autoxidation Involving Peroxy Radicals: A Key Contributor to Atmospheric Aerosol, *Chem. Rev.*, 119, 3472–3509, doi:10.1021/acs.chemrev.8b00395, 2019.

Carlton, A. G., Wiedinmyer, C. and Kroll, J. H.: A review of Secondary Organic Aerosol (SOA) formation from isoprene, *Atmos. Chem. Phys. Atmos. Chem. Phys.*, 9, 4987–5005 [online] Available from: www.atmos-chem-



- 320 phys.net/9/4987/2009/ (Accessed 23 January 2018), 2009.
- Carlton, A. G., Pye, H. O. T., Baker, K. R. and Hennigan, C. J.: Additional Benefits of Federal Air-Quality Rules: Model Estimates of Controllable Biogenic Secondary Organic Aerosol, *Environ. Sci. Technol.*, 52(16), 9254–9265, doi:10.1021/acs.est.8b01869, 2018.
- 325 Ceacero-Vega, A. A., Ballesteros, B., Bejan, I., Barnes, I., Jiménez, E. and Albaladejo, J.: Kinetics and Mechanisms of the Tropospheric Reactions of Menthol, Borneol, Fenchol, Camphor, and Fenchone with Hydroxyl Radicals (OH) and Chlorine Atoms (Cl), *J. Phys. Chem. A*, 116, 4097–4107, doi:10.1021/jp212076g, 2012.
- Chung, S. H. and Seinfeld, J. H.: Global distribution and climate forcing of carbonaceous aerosols, *J. Geophys. Res.*, 107(D19), 4407, doi:10.1029/2001JD001397, 2002.
- 330 Corchnoy, S. B. and Atkinson, R.: Kinetics of the gas-phase reactions of hydroxyl and nitrogen oxide (NO₃) radicals with 2-carene, 1,8-cineole, p-cymene, and terpinolene, *Environ. Sci. Technol.*, 24(10), 1497–1502, doi:10.1021/es00080a007, 1990.
- Després, V. R., Huffman, A. J., Burrows, S. M., Hoose, C., Safatov, A. S., Buryak, G., Fröhlich-Nowoisky, J., Elbert, W., Andreae, M. O., Pöschl, U. and Jaenicke, R.: Primary biological aerosol particles in the atmosphere: A review, *Tellus, Ser. B Chem. Phys. Meteorol.*, 64(1), doi:10.3402/tellusb.v64i0.15598, 2012.
- 335 Dudareva, N., Negre, F., Nagegowda, D. A. and Orlova, I.: Plant volatiles: Recent advances and future perspectives, *CRC. Crit. Rev. Plant Sci.*, 25(5), 417–440, doi:10.1080/07352680600899973, 2006.
- Ehn, M., Thornton, J. A., Kleist, E., Sipilä, M., Junninen, H., Pullinen, I., Springer, M., Rubach, F., Tillmann, R., Lee, B., Lopez-Hilfiker, F., Andres, S., Acir, I. H., Rissanen, M., Jokinen, T., Schobesberger, S., Kangasluoma, J., Kontkanen, J., Nieminen, T., Kurtén, T., Nielsen, L. B., Jørgensen, S., Kjaergaard, H. G., Canagaratna, M., Dal Maso, M., Berndt, T., Petäjä, T., Wahner, A., Kerminen, V. M., Kulmala, M., Worsnop, D. R., Wildt, J. and Mentel, T. F.: A large source of low-volatility secondary organic aerosol, *Nature*, 506, 476–479, doi:10.1038/Nature13032, 2014.
- 340 Faiola, C. L., Wen, M. and Vanreken, T. M.: Chemical characterization of biogenic secondary organic aerosol generated from plant emissions under baseline and stressed conditions: inter-and intra-species variability for six coniferous species, *Atmos. Chem. Phys.*, 15, 3629–3646, doi:10.5194/acp-15-3629-2015, 2015.
- 345 Faiola, C. L., Buchholz, A., Kari, E., Yli-Pirilä, P., Holopainen, J. K., Kivimäenpää, M., Miettinen, P., Worsnop, D. R., Lehtinen, K. E. J., Guenther, A. B. and Virtanen, A.: Terpene Composition Complexity Controls Secondary Organic Aerosol Yields from Scots Pine Volatile Emissions, *Nat. Sci. Reports*, 8(3053), doi:10.1038/s41598-018-21045-1, 2018.
- 350 Faiola, C. L., Pullinen, I., Buchholz, A., Khalaj, F., Ylisirniö, A., Kari, E., Miettinen, P., Holopainen, J. K., Kivimäenpää, M., Schobesberger, S., Yli-Juuti, T. and Virtanen, A.: Secondary Organic Aerosol Formation from Healthy and Aphid-Stressed Scots Pine Emissions, *ACS Earth Sp. Chem.*, doi:10.1021/acsearthspacechem.9b00118, 2019.
- 355 Fiore, A. M., Naik, V., Spracklen, D. V., Steiner, A., Unger, N., Prather, M., Bergmann, D., Cameron-Smith, P. J., Cionni, I., Collins, W. J., Dalsøren, S., Eyring, V., Folberth, G. A., Ginoux, P., Horowitz, L. W., Josse, B., Lamarque, J.-F., Mackenzie, I. A., Nagashima, T., O'Connor, F. M., Righi, M., Rumbold, S. T., Shindell, D. T., Skeie, R. B., Sudo, K., Szopa, S., Takemura, T. and Zeng, G.: Global air quality and climate, *Chem. Soc. Rev.*, 41, 6663–6683, doi:10.1039/c2cs35095e, 2012.
- 360 Forster, P., Ramaswamy, V., Artaxo, P., Berntsen, T., Betts, R., Fahey, D. W., Haywood, J., Lean, J., Lowe, D. C., Myhre, G., Nganga, J., Prinn, R., Raga, G., Schulz, M. and Van, R.: Changes in Atmospheric Constituents and in Radiative Forcing, in *Climate Change*, Cambridge University Press., 2007.
- Gaona-Colmán, E., Blanco, M. B., Barnes, I., Weisen, P. and Teruel, M. A.: OH- and O₃-initiated atmospheric



- degradation of camphene: temperature dependent rate coefficients, product yields and mechanisms, *RSC Adv.*, 7, 2733–2744, doi:10.1039/c6ra26656h, 2017a.
- 365 Gaona-Colmán, E., Blanco, M. B., Barnes, I., Weisen, P., Teruel, M. A., Colmán, C., María, M., Blanco, B., Barnes, I., Wiesen, P. and Teruel, M. A.: OH- and O₃-initiated atmospheric degradation of camphene: temperature dependent rate coefficients, product yields and mechanisms, *RSC Adv.*, 7, 2733–2744, doi:10.1039/c6ra26656h, 2017b.
- Gentner, D. R., Ormeño, E., Fares, S., Ford, T. B., Weber, R., Park, J.-H., Brioude, J., Angevine, W. M., Karlik, J. F. and Goldstein, A. H.: Emissions of terpenoids, benzenoids, and other biogenic gas-phase organic compounds from agricultural crops and their potential implications for air quality, *Atmos. Chem. Phys.*, 14, 5393–5413, doi:10.5194/acp-14-5393-2014, 2014.
- 370 Goldstein, A. H. and Galbally, I. E.: Known and unexplored organic constituents in the earth's atmosphere, *Environ. Sci. Technol.*, 41(5), 1514–1521, doi:10.1021/es072476p, 2007.
- Guenther, A.: Biological and Chemical Diversity of Biogenic Volatile Organic Emissions into the Atmosphere, *ISRN Atmos. Sci.*, (786290), doi:10.1155/2013/786290, 2013.
- 375 Guenther, A., Hewitt, C. N., Erickson, D., Guenther, A., Hewitt, N. C., Erickson, D., Fall, R., Geron, C., Graedel, T., Harley, P., Klinger, L., Lerdau, M., McKay, W. A., Pierce, T., Scholes, B., Steinbrecher, R., Tallamraju, R., Taylor, J. and Zimmerman, P.: A global model of natural volatile organic compound emissions, *J. Geophys. Res.*, 100(D5), 8873–8892, doi:10.1029/94JD02950, 1995.
- Guenther, A. B., Jiang, X., Heald, C. L., Sakulyanontvittaya, T., Duhl, T., Emmons, L. K. and Wang, X.: The Model of Emissions of Gases and Aerosols from Nature version 2.1 (MEGAN2.1): an extended and updated framework for modeling biogenic emissions, *Geosci. Model Dev.*, 5, 1471–1492, doi:10.5194/gmd-5-1471-2012, 2012.
- 380 Hall, W. A. and Johnston, M. V.: Oligomer Content of α -Pinene Secondary Organic Aerosol, *Aerosol Sci. Technol.*, 45(1), 37–45, doi:10.1080/02786826.2010.517580, 2011.
- Hao, L. Q., Yli-Pirilä, P., Tiitta, P., Romakkaniemi, S., Vaattovaara, P., Kajos, M. K., Rinne, J., Heijari, J., Kortelainen, A., Miettinen, P., Kroll, J. H., Holopainen, J. K., Smith, J. N., Joutsensaari, J., Kulmala, M., Worsnop, D. R. and Laaksonen, A.: New particle formation from the oxidation of direct emissions of pine seedlings, *Atmos. Chem. Phys.*, 9(20), 8121–8137, doi:10.5194/acp-9-8121-2009, 2009.
- 385 Hao, L. Q., Romakkaniemi, S., Yli-Pirilä, P., Joutsensaari, J., Kortelainen, A., Kroll, J. H., Miettinen, P., Vaattovaara, P., Tiitta, P., Jaatinen, A., Kajos, M. K., Holopainen, J. K., Heijari, J., Rinne, J., Kulmala, M., Worsnop, D. R., Smith, J. N. and Laaksonen, A.: Mass yields of secondary organic aerosols from the oxidation of α -pinene and real plant emissions, *Atmos. Chem. Phys.*, 11, 1367–1378, doi:10.5194/acp-11-1367-2011, 2011.
- Hoffmann, T., Odum, J. R., Bowman, F., Collins, D., Klockow, D., Flagan, R. C. and Seinfeld, J. H.: Formation of Organic Aerosols from the Oxidation of Biogenic Hydrocarbons, *J. Atmos. Chem.*, 26, 189–222, 1997.
- Huang, W., Saathoff, H., Pajunoja, A., Shen, X., Naumann, K.-H., Wagner, R., Virtanen, A., Leisner, T. and Mohr, C.: α -Pinene secondary organic aerosol at low temperature: chemical composition and implications for particle viscosity, *Atmos. Chem. Phys.*, 18(18), 2883–2898, doi:10.5194/acp-18-2883-2018, 2018.
- 395 Jimenez, J. L., Canagaratna, M. R., Donahue, N. M., Prevot, a. S. H., Zhang, Q., Kroll, J. H., DeCarlo, P. F., Allan, J. D., Coe, H., Ng, N. L., Aiken, a. C., Docherty, K. S., Ulbrich, I. M., Grieshop, A. P., Robinson, a. L., Duplissy, J., Smith, J. D., Wilson, K. R., Lanz, V. a., Hueglin, C., Sun, Y. L., Tian, J., Laaksonen, A., Raatikainen, T., Rautiainen, J., Vaattovaara, P., Ehn, M., Kulmala, M., Tomlinson, J. M., Collins, D. R., Cubison, M. J., Dunlea, J., Huffman, J. A., Onasch, T. B., Alfarra, M. R., Williams, P. I., Bower, K., Kondo, Y., Schneider, J., Drewnick, F., Borrmann, S., Weimer, S., Demerjian, K., Salcedo, D., Cottrell, L., Griffin, R., Takami, A., Miyoshi, T., Hatakeyama, S., Shimono, A., Sun, J. Y., Zhang, Y. M., Dzepina, K., Kimmel, J. R., Sueper, D., Jayne, J. T., Herndon, S. C., Trimborn, a. M., Williams, L. R., Wood, E. C., Middlebrook, A. M., Kolb, C. E., Baltensperger, U., Worsnop, D. R., Dunlea, E. J.,



- 405 Huffman, J. A., Onasch, T. B., Alfarra, M. R., Williams, P. I., Bower, K., Kondo, Y., Schneider, J., Drewnick, F., Borrmann, S., Weimer, S., Demerjian, K., Salcedo, D., Cottrell, L., Griffin, R., Takami, A., Miyoshi, T., Hatakeyama, S., Shimono, A., Sun, J. Y., Zhang, Y. M., Dzepina, K., Kimmel, J. R., Sueper, D., Jayne, J. T., Herndon, S. C., Trimborn, a. M., Williams, L. R., Wood, E. C., Middlebrook, A. M., Kolb, C. E., Baltensperger, U., Worsnop, D. R., Dunlea, J., Huffman, J. A., et al.: Evolution of Organic Aerosols in the Atmosphere, *Science* (80-.), 326, 1525–1529, doi:10.1126/science.1180353, 2009.
- 410 Jokinen, T., Sipilä, M., Richters, S., Kerminen, V. M., Paasonen, P., Stratmann, F., Worsnop, D., Kulmala, M., Ehn, M., Herrmann, H. and Berndt, T.: Rapid autoxidation forms highly oxidized RO₂ radicals in the atmosphere, *Angew. Chemie - Int. Ed.*, 53, 14596–14600, doi:10.1002/anie.201408566, 2014.
- Joutsensaari, J., Loivamäki, M., Vuorinen, T., Miettinen, P., Nerg, A.-M., Holopainen, J. K. and Laaksonen, A.:
415 Nanoparticle formation by ozonolysis of inducible plant volatiles, *Atmos. Chem. Phys.*, 5, 1489–1495, doi:10.5194/acp-5-1489-2005, 2005.
- Joutsensaari, J., Yli-Pirilä, P., Korhonen, H., Arola, A., Blande, J. D., Heijari, J., Kivimäenpää, M., Mikkonen, S., Hao, L., Miettinen, P., Lyytikäinen-Saarenmaa, P., Faiola, C. L., Laaksonen, A. and Holopainen, J. K.: Biotic stress accelerates formation of climate-relevant aerosols in boreal forests, *Atmos. Chem. Phys.*, 15(21), 12139–12157, doi:10.5194/acp-15-12139-2015, 2015.
- 420 Karban, R., Wetzal, W. C., Shiojiri, K., Ishizaki, S., Ramirez, S. R. and Blande, J. D.: Deciphering the language of plant communication: Volatile chemotypes of sagebrush, *New Phytol.*, 204, 380–385, doi:10.1111/nph.12887, 2014.
- Kourtchev, I., Giorio, C., Manninen, A., Wilson, E., Mahon, B., Aalto, J., Kajos, M., Venables, D., Ruuskanen, T., Levula, J., Loponen, M., Connors, S., Harris, N., Zhao, D., Kiendler-Scharr, A., Mentel, T., Rudich, Y., Hallquist, M.,
425 Doussin, J.-F., Maenhaut, W., Bäck, J., Petäjä, T., Wenger, J., Kulmala, M. and Kalberer, M.: Enhanced Volatile Organic Compounds emissions and organic aerosol mass increase the oligomer content of atmospheric aerosols, *Nat. Publ. Gr.*, 6(35038), doi:10.1038/srep35038, 2016.
- Kroll, J. H. E. AL: Secondary Organic Aerosol Formation from Isoprene Photooxidation, *Environ. Sci. Technol.*, 40, 1869–1877, doi:10.1021/es0524301, 2006.
- 430 Kundu, S., Fisseha, R., Putman, A. L., Rahn, T. A. and Mazzoleni, L. R.: High molecular weight SOA formation during limonene ozonolysis: insights from ultrahigh-resolution FT-ICR mass spectrometry characterization, *Atmos. Chem. Phys.*, 12, 5523–5536, doi:10.5194/acp-12-5523-2012, 2012.
- Lamarque, J.-F. F., Bond, T. C., Eyring, V., Granier, C., Heil, A., Klimont, Z., Lee, D., Liousse, C., Mieville, A., Owen, B., Schultz, M. G., Shindell, D., Smith, S. J., Stehfest, E., Van Aardenne, J., Cooper, O. R., Kainuma, M.,
435 Mahowald, N., McConnell, J. R., Naik, V., Riahi, K. and Van Vuuren, D. P.: Historical (1850–2000) gridded anthropogenic and biomass burning emissions of reactive gases and aerosols: Methodology and application, *Atmos. Chem. Phys.*, 10, 7017–7039, doi:10.5194/acp-10-7017-2010, 2010.
- Lambe, A., Massoli, P., Zhang, X., Canagaratna, M., Nowak, J., Daube, C., Yan, C., Nie, W., Onasch, T., Jayne, J., Kolb, C., Davidovits, P., Worsnop, D. and Brune, W.: Controlled nitric oxide production via O(1D) + N₂O reactions for use in oxidation flow reactor studies, *Atmos. Meas. Tech.*, 10, 2283–2298, doi:10.5194/amt-10-2283-2017, 2017.
- 440 Lambe, A. T., Ahern, A. T., Williams, L. R., Slowik, J. G., Wong, J. P. S., Abbatt, J. P. D., Brune, W. H., Ng, N. L., Wright, J. P., Croasdale, D. R., Worsnop, D. R., Davidovits, P. and Onasch, T. B.: Characterization of aerosol photooxidation flow reactors: heterogeneous oxidation, secondary organic aerosol formation and cloud condensation nuclei activity measurements, *Atmos. Meas. Tech.*, 4, 445–461, doi:10.5194/amt-4-445-2011, 2011.
- 445 Lee, B. H., Lopez-Hilfiker, F. D., Mohr, C., Kurtén, T., Worsnop, D. R., Thornton, J. A., Kurte, T., Worsnop, D. R., Thornton, J. A., Kurtén, T., Worsnop, D. R. and Thornton, J. A.: An iodide-adduct high-resolution time-of-flight chemical-ionization mass spectrometer: Application to atmospheric inorganic and organic compounds, *Environ. Sci. Technol.*, 48, 6309–6317, doi:10.1021/es500362a, 2014.



- Li, R., Palm, B. B., Ortega, A. M., Hlywiak, J., Hu, W., Peng, Z., Day, D. A., Knote, C., Brune, W. H., De Gouw, J.
450 A. and Jimenez, J. L.: Modeling the Radical Chemistry in an Oxidation Flow Reactor: Radical Formation and
Recycling, Sensitivities, and the OH Exposure Estimation Equation, *J. Phys. Chem. A*, 119, 4418–4432,
doi:10.1021/jp509534k, 2015.
- Lohmann, U. and Feichter, J.: Global indirect aerosol effects: a review, *Atmos. Chem. Phys.*, 5, 715–737 [online]
Available from: www.atmos-chem-phys.org/acp/5/715/ (Accessed 9 February 2017), 2005.
- 455 Lopez-Hilfiker, F. D., Mohr, C., Ehn, M., Rubach, F., Kleist, E., Wildt, J., Mentel, T. F., Lutz, A., Hallquist, M.,
Worsnop, D. and Thornton, J. A.: A novel method for online analysis of gas and particle composition: Description and
evaluation of a filter inlet for gases and AEROSols (FIGAERO), *Atmos. Meas. Tech.*, 7, 983–1001, doi:10.5194/amt-
7-983-2014, 2014.
- Lopez-Hilfiker, F. D., Iyer, S., Mohr, C., Lee, B. H., D’ambro, E. L., Kurtén, T. and Thornton, J. A.: Constraining the
460 sensitivity of iodide adduct chemical ionization mass spectrometry to multifunctional organic molecules using the
collision limit and thermodynamic stability of iodide ion adducts, *Atmos. Meas. Tech.*, 9, 1505–1512, doi:10.5194/amt-
9-1505-2016, 2016.
- McFiggans, G., Mentel, T. F., Wildt, J., Pullinen, I., Kang, S., Kleist, E., Schmitt, S., Springer, M., Tillmann, R., Wu,
C., Zhao, D., Hallquist, M., Faxon, C., Le Breton, M., Hallquist, Å. M., Simpson, D., Bergström, R., Jenkin, M. E.,
465 Ehn, M., Thornton, J. A., Alfarra, M. R., Bannan, T. J., Percival, C. J., Priestley, M., Topping, D. and Kiendler-Scharr,
A.: Secondary organic aerosol reduced by mixture of atmospheric vapours, *Nature*, 565, 587–593, doi:10.1038/s41586-
018-0871-y, 2019.
- Mentel, T. F., Wildt, J., Kiendler-Scharr, A., Kleist, E., Tillmann, R., Dal Maso, M., Fisseha, R., Hohaus, T., Spahn,
H., Uerlings, R., Wegener, R., Griffiths, P. T., Dinar, E., Rudich, Y. and Wahner, A.: Photochemical production of
470 aerosols from real plant emissions, *Atmos. Chem. Phys.*, 9, 4387–4406 [online] Available from: www.atmos-chem-phys.net/9/4387/2009/ (Accessed 20 January 2020), 2009.
- Peng, Z., Day, D. A., Stark, H., Li, R., Lee-Taylor, J., Palm, B. B., Brune, W. H. and Jimenez, J. L.: HO_x radical
chemistry in oxidation flow reactors with low-pressure mercury lamps systematically examined by modeling, *Atmos.*
Meas. Tech., 8, 4863–4890, doi:10.5194/amt-8-4863-2015, 2015.
- 475 Peng, Z., Palm, B. B., Day, D. A., Talukdar, R. K., Hu, W., Lambe, A. T., Brune, W. H. and Jimenez, J. L.: Model
Evaluation of New Techniques for Maintaining High-NO Conditions in Oxidation Flow Reactors for the Study of OH-
Initiated Atmospheric Chemistry, *ACS Earth Sp. Chem.*, 2, 72–86, doi:10.1021/acsearthspacechem.7b00070, 2018.
- Putman, A. L., Offenberg, J. H., Kundu, S., Rahn, T., Fisseha, R., Rahn, T. A. and Mazzoleni, L. R.: Ultrahigh-
480 resolution FT-ICR mass spectrometry characterization of a-pinene ozonolysis SOA, *Atmos. Environment*, 46, 164–172,
doi:10.1016/j.atmosenv.2011.10.003, 2011.
- Quéléver, L. L. J., Kristensen, K., Normann Jensen, L., Rosati, B., Teiwes, R., Daellenbach, K. R., Peräkylä, O., Roldin,
P., Bossi, R., Pedersen, H. B., Glasius, M., Bilde, M. and Ehn, M.: Effect of temperature on the formation of highly
oxygenated organic molecules (HOMs) from alpha-pinene ozonolysis, *Atmos. Chem. Phys.*, 19, 7609–7625,
doi:10.5194/acp-19-7609-2019, 2019.
- 485 Riva, M., Rantala, P., Krechmer, J. E., Peräkylä, O., Zhang, Y., Heikkinen, L., Garmash, O., Yan, C., Kulmala, M.,
Worsnop, D. and Ehn, M.: Evaluating the performance of five different chemical ionization techniques for detecting
gaseous oxygenated organic species, *Atmos. Meas. Tech.*, 12, 2403–2421, doi:10.5194/amt-12-2403-2019, 2019.
- Schobesberger, S., D’ambro, E. L., Lopez-Hilfiker, F. D., Mohr, C. and Thornton, J. A.: A model framework to retrieve
thermodynamic and kinetic properties of organic aerosol from composition-resolved thermal desorption measurements,
490 *Atmos. Chem. Phys.*, 18, 14757–14785, doi:10.5194/acp-18-14757-2018, 2018.
- Stark, H., Yatavelli, R. L. N., Thompson, S. L., Kang, H., Krechmer, J. E., Kimmel, J. R., Palm, B. B., Hu, W., Hayes,



- 495 P. L., Day, D. A., Campuzano-Jost, P., Canagaratna, M. R., Jayne, J. T., Worsnop, D. R. and Jimenez, J. L.: Impact of Thermal Decomposition on Thermal Desorption Instruments: Advantage of Thermogram Analysis for Quantifying Volatility Distributions of Organic Species, *Environ. Sci. Technol.*, 51, 8491–8500, doi:10.1021/acs.est.7b00160, 2017.
- Tolocka, M. P., Jang, M., Ginter, J. M., Cox, F. J., Kamens, R. M. and Johnston, M. V.: Formation of Oligomers in Secondary Organic Aerosol, *Environ. Sci. Technol.*, 38, 1428–1434, doi:10.1021/es035030r, 2004.
- Tu, P., Hall, W. A. and Johnston, M. V.: Characterization of Highly Oxidized Molecules in Fresh and Aged Biogenic Secondary Organic Aerosol, *Anal. Chem.*, 88, 4495–4501, doi:10.1021/acs.analchem.6b00378, 2016.
- 500 Tyson, B. J., Dement, W. A. and Mooney, H. A.: Volatilisation of terpenes from *Salvia mellifera*, *Nature*, 252(5479), 119–121, doi:10.1038/252119a0, 1974.
- Vanreken, T. M., Greenberg, J. P., Harley, P. C., Guenther, A. B. and Smith, J. N.: Direct measurement of particle formation and growth from the oxidation of biogenic emissions, *Atmos. Chem. Phys.*, 6, 4403–4413 [online] Available from: www.atmos-chem-phys.net/6/4403/2006/ (Accessed 10 February 2020), 2006.
- 505 Wyche, K. P., Ryan, A. C., Hewitt, C. N., Alfarra, M. R., Mcfiggans, G., Carr, T., Monks, P. S., Smallbone, K. L., Capes, G., Hamilton, J. F., Pugh, T. A. M. and Mackenzie, A. R.: Emissions of biogenic volatile organic compounds and subsequent photochemical production of secondary organic aerosol in mesocosm studies of temperate and tropical plant species, *Atmos. Chem. Phys.*, 14, 12781–12801, doi:10.5194/acp-14-12781-2014, 2014.
- 510 Yli-Pirilä, P., Copolovici, L., Kännaste, A., Noe, S., Blande, J. D., Mikkonen, S., Klemola, T., Pulkkinen, J., Virtanen, A., Laaksonen, A., Joutsensaari, J., Niinemets, Ü. and Holopainen, J. K.: Herbivory by an Outbreking Moth Increases Emissions of Biogenic Volatiles and Leads to Enhanced Secondary Organic Aerosol Formation Capacity, *Environ. Sci. Technol.*, 50(21), 11501–11510, doi:10.1021/acs.est.6b02800, 2016.
- Ylisirniö, A., Buchholz, A., Mohr, C., Li, Z., Barreira, L., Lambe, A., Kari, E., Yli-juuti, T., Nizkorodov, S. A., Worsnop, D. R. and Schobesberger, S.: Composition and volatility of SOA formed from oxidation of real tree emissions compared to single VOC-systems, *Atmos. Chem. Phys. Discuss.*, 1–29, 2019.
- 515 Zhang, X., Mcvay, R. C., Huang, D. D., Dalleska, N. F., Aumont, B., Flagan, R. C. and Seinfeld, J. H.: Formation and evolution of molecular products in α -pinene secondary organic aerosol, *Proc. Natl. Acad. Sci.*, 112(46), 14168–14173, doi:10.1073/pnas.1517742112, 2015.
- Zhao, D. F., Buchholz, A., Tillmann, R., Kleist, E., Wu, C., Rubach, F., Kiendler-Scharr, A., Rudich, Y., Wildt, J. and Mentel, T. F.: Environmental conditions regulate the impact of plants on cloud formation, *Nat. Commun.*, 8(1), 1–8, doi:10.1038/ncomms14067, 2017.